

## Study of heavy-lepton production in $e^+e^-$ annihilation

Kazuo Fujikawa\*

*Deutsches Elektronen-Synchrotron DESY, Hamburg, Germany*

Noboru Kawamoto

*Department of Physics, Tokyo Institute of Technology, Oh-okayama, Tokyo 152, Japan*

(Received 14 January 1976)

We present a numerical study of the collinearity-angle distribution for  $e$  and  $\mu$  in the process  $e\bar{e} \rightarrow L\bar{L}$  and the subsequent decay  $L \rightarrow \nu_L + l + \bar{\nu}_l$ ,  $l = \mu$  or  $e$ .  $V+A$  as well as  $V-A$  couplings for the heavy lepton are considered together with a nonvanishing mass for  $\nu_L$ . A  $V+A$  current with a massless or massive neutrino or a  $V-A$  current with a massive neutrino gives rise to more  $e\mu$  events at smaller collinearity angles than the standard  $V-A$  sequential lepton with a massless neutrino. A smaller heavy-lepton mass and larger experimental energy cutoff also give rise to smaller collinearity angles. It appears to be possible to distinguish these dynamical and kinematical effects based on experimental data with better statistics than available at present. We note that the experimental determination of the leptonic branching ratio is sensitive to the coupling scheme and the neutrino mass. We present an expected collinearity-angle distribution for  $l\pi$  events ( $l = \mu$  or  $e$ ), which may be conveniently used to fix the mass of  $\nu_L$ . The effects of the possible existence of heavy leptons on the decreasing charged energy fraction in  $e\bar{e}$  annihilation are also briefly discussed on the basis of recent data. A heavy lepton with mass  $\sim 1.8$  GeV can account for the decrease up to  $W \sim 6$  GeV. To explain the further decrease in the charged energy fraction *entirely* in terms of heavy leptons, however, another heavy lepton with mass  $\sim 2.8$  GeV accompanied by a massive neutrino is required. We comment on the effects of such heavier leptons on the  $e\mu$  cross section.

### I. INTRODUCTION

The most plausible interpretation of the  $e\mu$  events recently reported by Perl *et al.*<sup>1</sup> is that they are due to a (sequential) heavy lepton<sup>2</sup>  $L$  with a mass of about 1.8 GeV and an associated neutrino  $\nu_L$ .<sup>1</sup> A charged heavy lepton in this mass range also appears to be favored by the existing data on the rising ratio  $R$  and the decreasing charged energy fraction in  $e\bar{e}$  annihilation.<sup>3</sup>

In the present paper we continue the investigation of the effects of the possible existence of heavy leptons in  $e\bar{e}$  annihilation. The sequential heavy-lepton scheme<sup>2</sup> and its variant with an arbitrary combination of  $V$  and  $A$  charged currents will be adopted as the basis of our study. The effective Lagrangian is taken to be

$$L = (G/\sqrt{2})\bar{L}\gamma^\mu[\sin\alpha(1-\gamma_5) + \cos\alpha(1+\gamma_5)]\nu_L \\ \times \bar{\nu}_l\gamma_\mu(1-\gamma_5)l + \text{H.c.}, \quad (1.1)$$

with  $l = \mu$  or  $e$ . The parameter  $\alpha$  lies in  $-\frac{1}{2}\pi \leq \alpha \leq +\frac{1}{2}\pi$ , and  $|\alpha| = 0$  and  $\frac{1}{2}\pi$  correspond to  $V+A$  and  $V-A$  currents, respectively. The coupling constant  $G$  is assumed to be  $G \approx G_F$ , the Fermi constant, but only the lifetime is sensitive to the precise value of  $G$ . The neutrino accompanying the heavy lepton may also have a nonvanishing mass. We do not discuss those heavy leptons appearing in various gauge models.<sup>4</sup> All the formulas in Secs. III and IV are written for the general Lagrangian (1.1), but numerically we always compare  $V+A$  and  $V-A$  currents in the present paper.

### II. DECAY BRANCHING RATIOS OF HEAVY LEPTONS AND THE CHARGED ENERGY FRACTION IN $e^+e^-$

Here we tabulate the expected decay properties of heavy leptons and discuss the change in the charged energy fraction in  $e\bar{e}$  annihilation caused by those heavy leptons. The decay properties are also used in the following sections, where we discuss the dynamical properties of  $e\mu$  and  $l\pi$  events.

#### A. Decay properties

Estimates for various heavy-lepton decay modes have been discussed by many authors in the past.<sup>5</sup> On the basis of this general formalism we evaluated various decay modes elsewhere<sup>3</sup> and gave expected charged energy fractions for a 1.8-GeV heavy lepton. Here we extend this calculation to the case where (i) the current for the heavy lepton may be left- or right-handed, and (ii) the associated neutrino may be massive. The branching ratios are independent of whether one assumes a right-handed or a left-handed current for the heavy lepton. The charged energy fraction for the leptonic modes is slightly modified if one changes  $V-A$  to  $V+A$ . The charged energy fraction for hadronic modes is not modified by adopting  $V+A$  instead of  $V-A$  in the following approximate treatment. The result of these efforts is shown in Table I.

We briefly summarize the major assumptions involved in our estimates.<sup>5</sup> The hadronic weak spectral functions,  $\rho_1$  and  $\rho_2$ , are defined by

$$\sum_F \langle 0 | J_\mu^{W\dagger}(0) | F \rangle \langle F | J_\nu^W(0) | 0 \rangle (2\pi)^3 \delta(Q - P_F) \\ = \rho_1(s)(Q_\mu Q_\nu - Q^2 g_{\mu\nu}) + \rho_2(s)Q_\mu Q_\nu, \quad (2.1)$$

TABLE I. Relative decay width and charged energy fraction. The relative decay width is normalized to  $\Gamma \equiv G^2 M_L^5 / 192 \pi^3$ , the electronic decay width with a vanishing  $\nu_L$  mass for each  $M_L$ . The charged energy fraction for each decay mode is shown inside the parentheses. For leptonic decay modes, the first figure stands for a  $V-A$  current and the second for a  $V+A$  current. The charged energy fraction  $r_L$  is slightly smaller for a  $V+A$  current. All the charged particles in the final state are assumed to be pions when we estimate the charged energy fraction. The parameters  $r_L$  and  $\delta$  are defined in Eq. (2.15).

	$M_L = 1.8 \text{ GeV}$ $m_{\nu_L} = 0$	$M_L = 1.8 \text{ GeV}$ $m_{\nu_L} = 0.54 \text{ GeV}$	$M_L = 2.8 \text{ GeV}$ $m_{\nu_L} = 1.4 \text{ GeV}$
$L \rightarrow \nu_L + e + \bar{\nu}_e$	1.00 (0.35, 0.30)	0.52 (0.29, 0.26)	0.16 (0.22, 0.20)
$L \rightarrow \nu_L + \mu + \bar{\nu}_\mu$	1.00 (0.35, 0.30)	0.52 (0.29, 0.26)	0.16 (0.22, 0.20)
$L \rightarrow \nu_L + \pi$	0.55 (0.50)	0.41 (0.45)	0.10 (0.38)
$L \rightarrow \nu_L + K$	0.02 (0.46)	0.017 (0.42)	0.004 (0.35)
$L \rightarrow \nu_L + \rho$	1.20 (0.30)	0.86 (0.27)	0.22 (0.21)
$L \rightarrow \nu_L + K^*$	0.06 (0.25)	0.04 (0.23)	0.01 (0.18)
$L \rightarrow \nu_L + A_1$	0.44 (0.46)	0.24 (0.44)	0.08 (0.31)
$L \rightarrow \nu_L + \text{hadron continuum}$	0.97 (0.44)	0.25 (0.38)	0.13 (0.27)
Total	5.24	2.86	0.86
$\nu_L + \text{hadrons}$	3.24 (0.40)	1.82 (0.35)	0.54 (0.28)
$r_L(V-A)$	0.39	0.34	0.27
$\delta$	0.9	0.9	0.9
$\frac{\Gamma(L \rightarrow \nu_L + e + \bar{\nu}_e)}{\Gamma(L \rightarrow \text{all})}$	0.19	0.18	0.19

and the following assumptions are made:

(i) The electron and muon masses can be ignored.

(ii) Single-particle contributions can be estimated on the basis of the parametrization: For  $X = \pi, K$ ,

$$\rho_1^X = 0, \quad \rho_2^X = f_X^2 \delta(s - m_X^2); \quad (2.2)$$

For  $X = \rho, K^*, A_1$ ,

$$\rho_1^X = 2m_X^2 / \gamma_X^2 \delta(s - m_X^2), \quad \rho_2^X = 0, \quad (2.3)$$

together with the second Weinberg sum rule<sup>6</sup>

$$\gamma_\rho / m_\rho^2 = \gamma_{A_1} / m_{A_1}^2, \quad (2.4)$$

the Das-Mathur-Okubo sum rule<sup>7</sup>

$$\gamma_\rho / m_\rho = \gamma_{K^*} / m_{K^*}, \quad (2.5)$$

$$\frac{\Gamma(L \rightarrow \nu_L + \text{hadron continuum})}{\Gamma(L \rightarrow \nu_L + e + \bar{\nu}_e)}$$

$$\cong \frac{3}{M^8} \int_{s_c}^{(M-m)^2} ds \lambda(M^2, m^2, s) s R(s) \left\{ 2(M^2 + m^2 - s) + \frac{1}{s} [(M^2 + m^2)(M^2 + m^2 - s) - 4M^2 m^2] \right\}, \quad (2.9)$$

where

$$\lambda(M^2, m^2, s) = (M^4 + m^4 + s^2 - 2M^2 s - 2m^2 s - 2M^2 m^2)^{1/2}, \quad (2.10)$$

with  $M$  and  $m$  the masses for  $L$  and  $\nu_L$ , respectively. The parameter  $s_c$  is the smallest invariant mass of hadrons which contribute to the decay

$$L \rightarrow \nu_L + \text{hadron continuum}. \quad (2.11)$$

The value of  $s_c$  is taken at 1 (GeV)<sup>2</sup> in our esti-

and experimental values<sup>8</sup>:

$$f_\pi \approx f_K \approx 0.9 m_\pi, \quad \gamma_\rho^2 / 4\pi \approx 2.5, \quad (2.6)$$

and

$$\sin\theta_c \approx 0.22. \quad (2.7)$$

(iii) The hadronic continuum can be treated by assuming conserved vector current (CVC), asymptotic chiral symmetry, and asymptotic SU(3) [or SU(4)] symmetry.<sup>5</sup> Then

$$\lim_{s \rightarrow \infty} \rho_1(s) = \frac{1}{4\pi^2} \lim_{s \rightarrow \infty} R(s), \quad (2.8)$$

$$R(s) \equiv \frac{\sigma(e\bar{e} \rightarrow \text{hadrons})}{\sigma(e\bar{e} \rightarrow \mu\bar{\mu})},$$

and we have<sup>2</sup>

mate. We also take<sup>9</sup>

$$R(s) \approx 1.5 \text{ for } 1 \leq s \leq (M-m)^2. \quad (2.12)$$

Now we turn to the charged energy fraction in  $L$  decay, which can be estimated from the known decay modes of these particles. For the hadronic

continuum, the neutrino is expected to carry away an average energy

$$\bar{E}_\nu \approx \frac{\int_m^{(M^2 - s_c)^{1/2}} dE E g(E) R(M^2 + m^2 - 2ME)}{\int_m^{(M^2 - s_c)^{1/2}} dE g(E) R(M^2 + m^2 - 2ME)}, \quad (2.13)$$

where (valid both for  $V-A$  and  $V+A$  couplings)

$$g(E) = (E^2 - m^2)^{1/2} [-4E^2 + 3(E/M)(M^2 + m^2) - 2m^2] \quad (2.14)$$

is the energy spectrum of the neutrino  $\nu_L$  for the *leptonic* decay mode in the rest frame of  $L$ , and  $R(s)$  is the ratio  $R$  in  $e\bar{e}$  annihilation. The charged hadrons are assumed to carry approximately 58% of the residual energy. [See Eq. (2.16) below.] The charged energy fraction for the leptonic mode is easily evaluated using the known energy spectrum of charged leptons. A left-handed current tends to give rise to more energetic  $\mu$  or  $e$ .

#### B. Charged energy fraction in $e\bar{e}$ annihilation

As we have shown elsewhere,<sup>3</sup> a heavy lepton with a mass of  $\approx 1.8$  GeV gives rise to a decrease in the charged energy fraction in  $e\bar{e}$  annihilation, which is of the same order of magnitude as the experimental decrease starting at  $W \sim 3.6$  GeV.<sup>9</sup> However, the newer data reported at the Stanford conference<sup>10</sup> show a less dramatic change in the charged energy fraction in the energy region. They also indicate that the charged energy fraction continues to decrease beyond 5 GeV up to the maximum available energy  $W \sim 8$  GeV. Because of this experimental development, we would like to re-examine the effects of heavy leptons on the decreasing charged energy fraction.

The charged energy fraction is given by

$$r_{ob}(W) = \frac{r_h(W)R_h(W) + r_L \frac{1}{2}\beta(3 - \beta^2)\delta}{R_h(W) + \frac{1}{2}\beta(3 - \beta^2)\delta}, \quad (2.15)$$

where  $R_h(W)$  is the hadronic contribution to the ratio  $R$ , and

$r_h(W)$  = charged energy fraction for the hadronic events,

$r_L$  = charged energy fraction in the heavy lepton for the decay modes  $hh$ ,  $h\mu$ ,  $he$ , and  $\mu\mu$ ,

$\delta \approx 0.9$  = total branching ratio for the above four decay modes of  $L$ , and

$$\beta \equiv (1 - 4M^2/W^2)^{1/2}.$$

Here the  $\mu h$  decay mode of  $L$ , e.g., stands for the combined process  $L^+ \rightarrow \mu^+ + \nu_\mu + \bar{\nu}_L$  and  $L^- \rightarrow \nu_L + \mu^- + \text{hadrons}$ , and the process where  $L^+$  and  $L^-$  are interchanged.

In Fig. 1 we show the values of  $r_{ob}(W)$  which are based on

$$r_h(W) \approx 0.58 \text{ for } W \geq 3.6 \quad (2.16)$$

and

$$r_L \approx 0.39 \text{ for } m = 0, \quad (2.17)$$

$$r_L \approx 0.34 \text{ for } m = 0.3M. \quad (2.18)$$

See also Table I. We observe that the heavy lepton with  $M = 1.8$  GeV can almost account for the decrease in the charged energy fraction up to  $W \sim 6$  GeV. However, it is difficult to explain the further decrease in the charged energy fraction at higher energies on the basis of single-heavy-lepton production. This may be an indication that the charged energy fraction for hadronic events also decreases with energy  $W$ , contrary to our ansatz (2.16).

However, it is also interesting to ask whether the further decrease of the charged energy fraction can be explained *entirely* in terms of heavy leptons by assuming another heavy lepton. In this case Fig. 1 indicates that another heavy lepton with a mass  $\sim 2.8$  GeV may be needed to explain the departure of the theoretical values from the decreasing values of the experimental charged energy fraction. Another constraint on the mass assignment comes from the experimental observation of  $e\mu$  events. If one assumes that the associated neutrino for  $L'$  at  $\sim 2.8$  GeV is massless, the experimental  $e\mu$  cross section must show a substantial increase around  $W = 5.5$  GeV. This is apparently not the case.<sup>1</sup> To satisfy these conditions, we tentatively take the second set of heavy leptons at

$$\begin{aligned} M_{L'} &\approx 2.8 \text{ GeV}, \\ m_{\nu_{L'}} &\approx 1.4 \text{ GeV}. \end{aligned} \quad (2.19)$$

The effects of these leptons on the  $e-\mu$  cross sec-

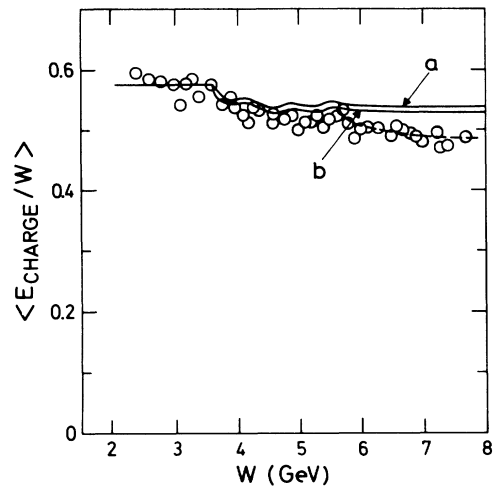


FIG. 1. Expected decrease in the charged energy fraction due to heavy leptons. (a)  $M = 1.8$  GeV,  $m_{\nu_L} = 0$ , (b)  $M = 1.8$  GeV,  $m_{\nu_L} = 540$  MeV. The dashed line stands for the effects of  $L'$  with  $M_{L'} = 2.8$  GeV and  $m_{\nu_{L'}} = 1.4$  GeV. The data are taken from Ref. 10.

tion will be commented on in the next section. The formula for the charged energy fraction (2.15) is now generalized to

$$r_{ob}(W) = \frac{r_h(W)R_h(W) + r_L \frac{1}{2}\beta(3 - \beta^2)\delta + r_{L'} \frac{1}{2}\beta'(3 - \beta'^2)\delta'}{R_h(W) + \frac{1}{2}\beta(3 - \beta^2)\delta + \frac{1}{2}\beta'(3 - \beta'^2)\delta'}, \quad (2.20)$$

and the observed value of the ratio  $R$  (see Refs. 10 and 11) is given by

$$R_{ob}(W) = R_h(W) + \frac{1}{2}\beta(3 - \beta^2)\delta + \frac{1}{2}\beta'(3 - \beta'^2)\delta'. \quad (2.21)$$

The estimates of  $r_{L'}$  and  $\delta'$  are shown in Table I. We show the charged energy fraction based on (2.20) by a dotted line in Fig. 1. The result now appears to account for the decreasing charged energy fraction up to  $W \sim 8$  GeV.

We close by noting that the global properties of  $e^*e^-$  ( $R$  and the charged energy fraction) are quite consistent with the assumption that  $L^*L^-$  are produced at present energies.

*Note added in proof.* After submitting the present paper, we learned that Schwitters<sup>10</sup> states in the written version of his talk at the Stanford Conference that the data of the charged-energy fraction are based on the events with more than two charged prongs. This event criterion, which was not clearly stated in Richter's talk at the London Conference,<sup>9</sup> has important effects on the analysis of the charged energy fraction:

(a) Our estimate of the fraction of events with more than two charged particles in heavy-lepton pair production is about 40% (or  $\sim 20\%$  in the decay rate of  $L$ ). This lowers the parameter  $\delta$  in (2.15) by a factor of 2. The effects of the possible existence of charged heavy leptons on the existing data of the charged energy fraction therefore become about one-half of our estimate.

(b) The nearly monotonic decrease of the charged-energy fraction up to  $\sim 8$  GeV may partly be due to this event criterion for purely hadronic

events. At low energies, where the total multiplicity is small, the events with more than two charged prongs mean that one selectively picks up those events with a relatively large charged energy fraction. This bias gradually disappears at higher energies.

We thank Professor H. Meyer for calling the above event criterion to our attention.

### III. ANOMALOUS LEPTON PRODUCTION

Assuming that the  $e\mu$  events in  $e\bar{e}$  annihilation reported by Perl *et al.*<sup>1</sup> are due to production and decay of a 1.8-GeV heavy lepton  $L$ , we discuss in some detail the consequences of different weak-coupling schemes on the experimental distributions.

#### A. Energy spectrum of the electron and the muon

The energy spectrum of the electron decaying from a moving heavy lepton in Fig. 2 is given by

$$\frac{d\Gamma}{dx} = \frac{1}{\beta} \left[ F\left(1 - \frac{2x}{1+\beta}\right) - F(\epsilon^2) \right] \quad (3.1)$$

for

$$\frac{1 - \epsilon^2}{2}(1 - \beta) \leq x \leq \frac{1 - \epsilon^2}{2}(1 + \beta), \quad (3.2)$$

and

$$\frac{d\Gamma}{dx} = \frac{1}{\beta} \left[ F\left(1 - \frac{2x}{1+\beta}\right) - F\left(1 - \frac{2x}{1-\beta}\right) \right]$$

for

$$0 \leq x \leq \frac{1 - \epsilon^2}{2}(1 - \beta).$$

Here  $x$  is the Feynman  $x$  variable defined by  $x \equiv 2E/W = E/M\gamma$ .  $M$ ,  $\beta$ , and  $\gamma$  are the mass and the Lorentz factors of the heavy lepton, respectively, and  $\epsilon$  is the ratio of the  $\nu_L$  mass to the  $L$  mass,  $\epsilon \equiv m/M$ . The lower end of the  $x$  distribution in (3.2) is slightly modified for the case of the muon. The function  $F(y)$  corresponding to the effective Lagrangian (1.1) is given by

$$F(y) = \frac{2}{N} \left\{ \cos^2\alpha \left[ -2y^3 + 3(1 + 2\epsilon^2)y^2 - 6\epsilon^2(2 + \epsilon^2)y + 6\epsilon^4 \ln y \right] + \sin^2\alpha \left[ -\frac{2}{3}y^3 + \left( \frac{1 + 3\epsilon^2}{2} \right) y^2 + (1 - 3\epsilon^2)y + \epsilon^4(3 - \epsilon^2) \ln y + \epsilon^4(3 + \epsilon^2)/y - \epsilon^6/y^2 \right] + \frac{\sin 2\alpha}{2} \epsilon \left[ 3y^2 - 6(1 + 2\epsilon^2)y + 6\epsilon^2(2 + \epsilon^2) \ln y + 6\epsilon^4/y \right] \right\}, \quad (3.3)$$

where

$$N \equiv f(\epsilon) + \sin 2\alpha g(\epsilon), \quad (3.4)$$

with

$$f(\epsilon) \equiv (1 - \epsilon^4)(1 - 8\epsilon^2 + \epsilon^4) - 24\epsilon^4 \ln \epsilon, \quad (3.5)$$

$$g(\epsilon) \equiv -2\epsilon \left[ (1 - \epsilon^2)(1 + 10\epsilon^2 + \epsilon^4) \right.$$

$$\left. + 12\epsilon^2(1 + \epsilon^2) \ln \epsilon \right]. \quad (3.6)$$

Incidentally, the leptonic width of  $L$  based on the

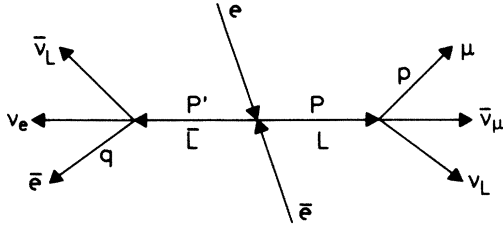


FIG. 2. Heavy-lepton production in  $e\bar{e}$  annihilation. The collinearity angle  $\theta$  is defined by  $\cos\theta \equiv -(\vec{p} \cdot \vec{q})/|\vec{p}||\vec{q}|$ .

Lagrangian (1.1) is given in terms of  $N$  in (3.4) as

$$\Gamma(L \rightarrow \nu_L + e + \bar{\nu}_e) = \frac{G^2 M^5}{192\pi^3} N.$$

Equation (3.1) assumes a scale-invariant form in terms of  $z = 2x/(1+\beta)$ , which approaches  $x$  at high energies,

$$\frac{2\beta}{1+\beta} \frac{d\Gamma}{dz} = [F(1-z) - F(\epsilon^2)]$$

for

$$(1 - \epsilon^2) \frac{1 - \beta}{1 + \beta} \leq z \leq 1 - \epsilon^2. \quad (3.7)$$

In Fig. 3 we show the energy spectrum for  $M=1.8$  GeV and  $W=4.8$  GeV. From this figure we observe the following:

(a) A neutrino  $\nu_L$  with a mass  $m \leq 500$  MeV or so does not significantly modify the energy spectrum. However, the value of  $\epsilon = m/M = 0.5$  appears to be too large, and it may be excluded by the present experimental data.<sup>12</sup>

(b) The energy spectrum for a  $V-A$  current with  $\epsilon=0.3$  and the energy spectrum for a  $V+A$  current with  $\epsilon=0$  are almost identical except at the upper end of the spectrum.

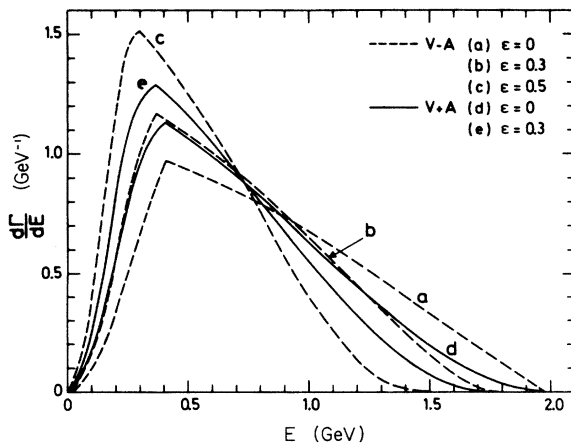


FIG. 3. Electron energy spectrum for  $M=1.8$  GeV and  $W=4.8$  GeV. The parameter  $\epsilon$  is the ratio of  $\nu_L$  mass to  $L$  mass,  $\epsilon = m_{\nu_L}/M$ .

On the basis of property (a) above, we always compare the cases  $\epsilon=0$  and  $\epsilon=0.3$  in the following. Values of  $\epsilon$  much smaller than 0.3 give rise to results almost indistinguishable from  $\epsilon=0$  for almost all the distributions in  $e\mu$  events. Property (b), which is valid at almost all energies [see (3.7)], indicates that it may be difficult to distinguish a  $V+A$  current from a  $V-A$  current if one allows a massive neutrino  $\nu_L$ .

### B. Collinearity-angle distribution

One of the dynamical quantities which characterize the  $e\mu$  events is the collinearity-angle distribution.<sup>1,12,13</sup> Some of the interesting properties of this distribution have been reported elsewhere.<sup>3</sup> An analytical formula, which may be useful at high energies, has also been given.<sup>14</sup> Here we present a detailed numerical analysis of this problem at lower energies.

As in Ref. 3, we assume a  $4\pi$  detector and no cutoffs in the collinearity angle in the following discussions. The heavy lepton has a rather uniform angular distribution with respect to the incident beam direction at low energies. The  $4\pi$ -counter approximation is therefore expected to be good for the large solid angle detectors at SPEAR and DORIS.<sup>1</sup> An (approximate)  $4\pi$  detector will after all be required in future experiments if one wants to make sure that there are no particles other than  $e$ ,  $\mu$ , and neutrinos in the final state. The noncoplanarity cutoff in the existing data<sup>1,12</sup> eliminates the collinearity-angle distribution for  $\theta \leq 20^\circ$ , and it partly modifies the distribution for  $\cos\theta \geq 0.7$ . As one can see in the following, it is much easier to distinguish various dynamical effects if the experimental data with a noncollinearity cutoff instead of the noncoplanarity cutoff become available. We note that our result in the following is *exact* for any noncollinearity cutoff with a  $4\pi$  detector.

The assumption of a  $4\pi$  detector means that we can calculate the normalized collinearity-angle distribution by first taking the average over the directions of the *incident*  $e^+e^-$  with the final-state configuration fixed.<sup>3</sup> The effects of the polarization of the incident electron beam disappear during this averaging procedure. This statement, which is valid in the one-photon approximation, can be proved by using the gauge invariance of electromagnetic current operators. Our result in the following, which is based on an unpolarized beam, is also applicable to the case of a polarized beam if one assumes an (approximate)  $4\pi$  detector.

After this angular averaging, the normalized distribution for  $\mu$  and  $e$  in Fig. 2, based on the Lagrangian (1.1), is given by (we neglect the muon mass)

$$d\Gamma = \frac{1}{N}(T_1 + T_2) \left( \frac{s - m^2}{s} \right) \left( \frac{s' - m^2}{s'} \right) \frac{d^3p}{2p_0} \frac{d^3q}{2q_0} \delta((P - p)^2 - s) \delta((P' - q)^2 - s') ds ds', \quad (3.8)$$

where

$$T_1 = \left( \frac{W^2 + 2M^2}{2M^2} \right) F(s) F(s'), \quad (3.9)$$

$$T_2 = 4G(s)G(s') \left[ M^2(p \cdot q) - (P' \cdot p)(P' \cdot q) - (P \cdot p)(P \cdot q) + \left( \frac{W^2 - 2M^2}{2M^2} \right) (P \cdot p)(P' \cdot q) \right], \quad (3.10)$$

with  $M$  and  $m$  the masses of  $L$  and  $\nu_L$ , respectively, and

$$F(s) \equiv (M^2 - s) \left[ \cos^2 \alpha (s - m^2) + \frac{\sin^2 \alpha}{6} \left( 1 - \frac{m^2}{s} \right) (2s + M^2 + m^2 + 2m^2 M^2/s) - \frac{\sin 2\alpha}{2} mM \left( 1 - \frac{m^2}{s} \right) \right], \quad (3.11)$$

$$G(s) \equiv \cos^2 \alpha (s - m^2) - \frac{\sin^2 \alpha}{6} \left( 1 - \frac{m^2}{s} \right) (2s - M^2 + m^2 - 2m^2 M^2/s) - \frac{\sin 2\alpha}{2} mM \left( 1 - \frac{m^2}{s} \right). \quad (3.12)$$

The normalization factor  $N$  is given by

$$N \equiv \left( \frac{W^2 + 2M^2}{2M^2} \right) \left( \frac{\pi M^6}{24} \right)^2 [f(\epsilon) + \sin 2\alpha g(\epsilon)]^2. \quad (3.13)$$

The functions  $f(\epsilon)$  and  $g(\epsilon)$  are given in Eqs. (3.5) and (3.6). The definition of various momenta is shown in Fig. 2, and the center-of-mass energy squared is denoted by  $W^2 = (P + P')^2$ . The variables  $s$  and  $s'$  correspond to the invariant mass of the  $\nu_L \bar{\nu}_\mu$  and  $\bar{\nu}_L \nu_e$  system, respectively. The *natural* phase-space boundaries are provided by

$$m^2 \leq s \leq M^2 \text{ and } m^2 \leq s' \leq M^2, \quad (3.14)$$

with  $M$  and  $m$  the masses of  $L$  and  $\nu_L$ , respectively.  $T_2$  in (3.8) stands for the spin alignment term.<sup>13</sup> The formula (3.8) is applicable only to the *relative* distributions among the final-state particles such as the  $e\mu$  collinearity-angle distribution. The collinearity-angle distribution in  $\cos\theta$  is defined by

$$\frac{d\Gamma}{d\cos\theta} \equiv \int d\Gamma \delta(\cos\theta + (\vec{p} \cdot \vec{q})/|\vec{p}||\vec{q}|). \quad (3.15)$$

In Ref. 3,  $d\Gamma/d\theta$  instead of  $d\Gamma/d\cos\theta$  was given following the convention in the preliminary analysis of the experimental data.<sup>1</sup> In general one can reduce the phase-space integration in (3.15) to a two-dimensional angular integration when one imposes energy cutoffs,  $p_0 \geq E_c$  and  $q_0 \geq E_c$ . The remaining two-dimensional integration in our case has been done numerically. A brief discussion of phase-space constraints is given in Appendix A. The numerical results are shown in Figs. 4–8. We observe the following characteristic properties:

(i) The distribution for a  $V+A$  current tends to be concentrated toward smaller values of  $\theta$  compared with that for a  $V-A$  current if all other parameters are identical.

(ii) The distributions given by a  $V-A$  current for  $E_c = 0.65$  GeV and  $\epsilon = 0.3$ , and for  $E_c = 0.75$  GeV and  $\epsilon = 0$  are very similar for  $M = 1.8$  GeV and  $W = 4.8$  GeV (see Fig. 4). This relation also applies to a  $V+A$  current in Fig. 5 (in fact, these two cases for a  $V+A$  current are hardly distinguishable). See also the lower end of the momentum distribution in Ref. 1.

(iii) The fraction of the  $e\mu$  events with energy greater than the cutoff energy  $E_c$  is obtained by integrating the collinearity-angle distribution

$$f \equiv \int \frac{d\Gamma}{d\cos\theta} d\cos\theta. \quad (3.16)$$

This  $f$  is approximately proportional to the acceptance of the detector system. The values of  $f$  for  $V-A$  and  $V+A$  currents at  $W = 4.8$  GeV respectively are obtained from Figs. 4 and 5 as

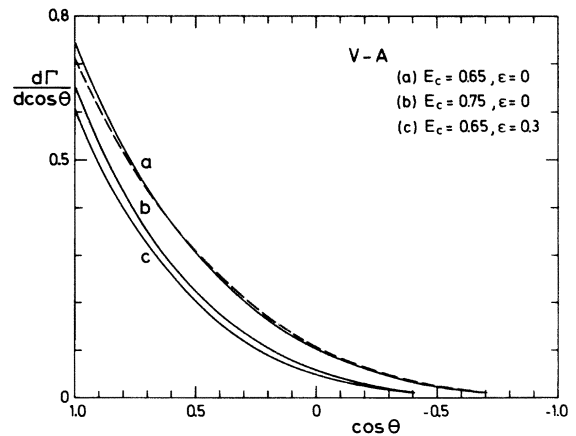


FIG. 4. Collinearity-angle distribution of  $e$  and  $\mu$  for a  $V-A$  current at  $W = 4.8$  GeV and  $M = 1.8$  GeV. The dashed line stands for the distribution corresponding to (a) but without the spin-alignment term.  $\epsilon = m_{\nu_L}/M$ , and  $E_c$  stands for the cutoff energy in GeV.

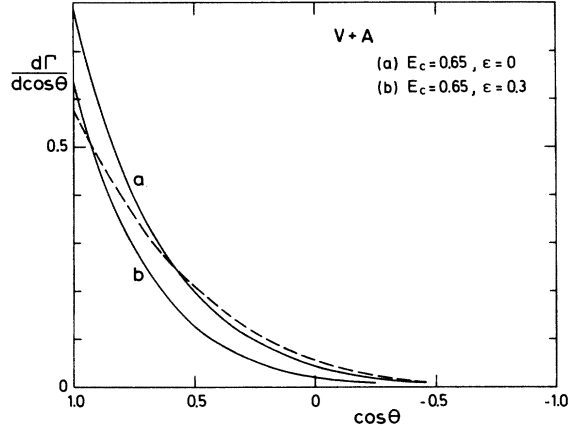


FIG. 5. Collinearity-angle distribution of  $e$  and  $\mu$  for a  $V+A$  current at  $W=4.8$  GeV and  $M=1.8$  GeV. The dashed line stands for the distribution corresponding to (a) but without the spin-alignment term.  $\epsilon=m_{\nu_L}/M$ , and  $E_c$  stands for the cutoff energy in GeV.

$$\begin{aligned} f &= 0.38 \text{ and } 0.28 \text{ for } E_c = 0.65 \text{ GeV and } \epsilon = 0, \\ f &= 0.25 \text{ and } 0.19 \text{ for } E_c = 0.65 \text{ GeV and } \epsilon = 0.3, \\ f &= 0.28 \text{ and } 0.19 \text{ for } E_c = 0.75 \text{ GeV and } \epsilon = 0. \end{aligned} \quad (3.17)$$

Namely, a  $V-A$  current (the first figures) gives rise to a larger  $e\mu$  signal than a  $V+A$  current. This is what we expect from the energy spectrum in Fig. 3. This difference has an important physical consequence. The relative leptonic branching ratio determined by the experimental observation of  $e\mu$  events is inversely proportional to the

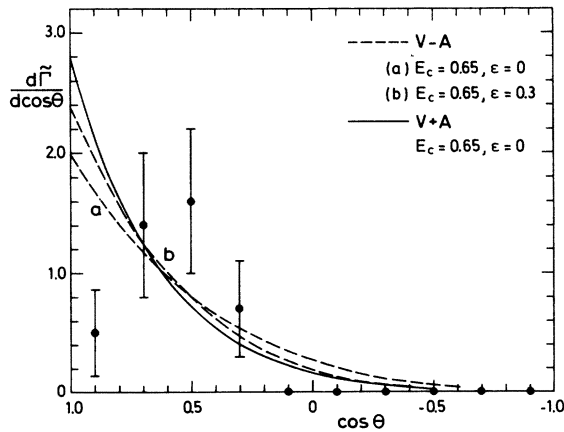


FIG. 6. Collinearity-angle distribution of  $e$  and  $\mu$  normalized to a unit area for  $W=4.8$  GeV and  $M=1.8$  GeV. The experimental data from Ref. (1) are also shown for the sake of comparison. Our curves do not include the effects of the noncoplanarity cutoff which modify the theoretical curves for  $\cos\theta \gtrsim 0.7$ .  $\epsilon=m_{\nu_L}/M$ , and  $E_c$  stands for the cutoff energy in GeV.

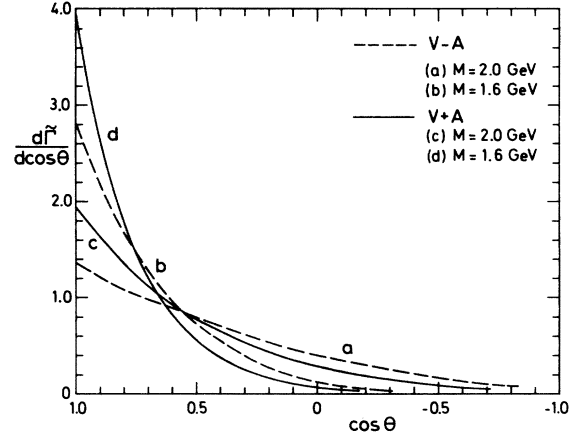


FIG. 7. Mass dependence of the collinearity-angle distribution of  $e$  and  $\mu$  at  $W=4.8$  GeV. The cutoff energy is taken at  $E_c = 0.65$  GeV. The area under the curve is normalized to unity.  $\epsilon=m_{\nu_L}/M=0$  for all the curves.

*theoretical estimate* of the counter acceptance. This means that the experimental value of  $\Gamma(L \rightarrow \nu_L + e + \bar{\nu}_e)/\Gamma(L \rightarrow \text{all}) \approx 15\%$  determined from a  $V-A$  current with a vanishing neutrino mass<sup>1</sup> is modified to

$$\Gamma(L \rightarrow \nu_L + e + \bar{\nu}_e)/\Gamma(L \rightarrow \text{all}) \approx 15 \times \left( \frac{0.38}{0.28} \right)^{1/2} \approx 18\% \quad (3.18)$$

for a  $V+A$  current with  $\epsilon=0$  or for a  $V-A$  current with  $\epsilon=0.3$ . It is amusing that this modified value is more consistent with our estimate in Table I.

(iv) To investigate the effects of the spin-alignment term<sup>13</sup>  $T_2$  in (3.8), the results without the spin-alignment term are shown by a dashed line in Figs. 4 and 5. The effects of spin alignment are small for a  $V-A$  current,<sup>3</sup> but significant for a

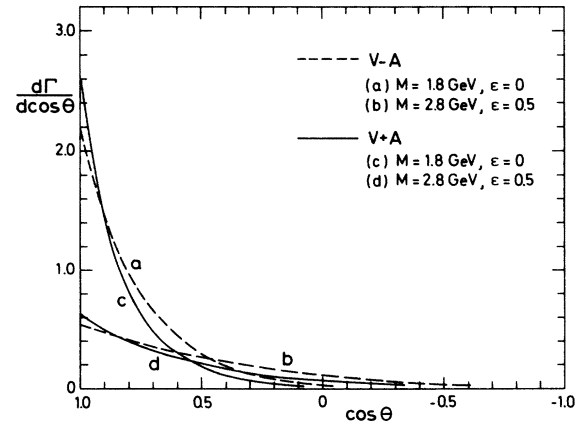


FIG. 8. Collinearity-angle distribution of  $e$  and  $\mu$  at  $W=7$  GeV. The cutoff energy is taken at  $E_c = 0.65$  GeV,  $\epsilon=m_{\nu_L}/M$ .

$V+A$  current. We note that both the shape and magnitude of the collinearity-angle distributions for  $V+A$  and  $V-A$  currents are different even without the spin-alignment term. This is a reflection of the different lepton energy spectra in Fig. 3 which depend on  $V-A$  or  $V+A$  coupling. This difference without the spin alignment term disappears for the vanishing energy cutoff,  $E_c=0$ .

(v) To discriminate the  $V-A$  and  $V+A$  currents, it may be convenient to normalize the area under the collinearity-angle distribution. Namely we define

$$\frac{d\bar{\Gamma}}{d\cos\theta} \equiv \frac{1}{f} \frac{d\Gamma}{d\cos\theta} \quad (3.19)$$

with  $f$  in (3.16). These normalized distributions are shown in Fig. 6. Here the experimental values<sup>1,12</sup> are also shown. As one can see, the present experimental data are not sufficient to make any definite statement about the dynamics. (The sharp decrease of the experimental values at small  $\theta$  is due to the noncoplanarity cutoff at  $\theta \simeq 20^\circ$ .) However, if one takes seriously the suppression of the data for  $\theta \gtrsim 90^\circ$  (which was emphasized in Ref. 1), a  $V+A$  current or a  $V-A$  current with  $\epsilon=0.3$  agrees better with the data.

(vi) The collinearity-angle distribution is also sensitive to the precise value of the heavy-lepton mass.<sup>3</sup> This is shown in Fig. 7. It is therefore important to first fix the heavy-lepton mass precisely before one discusses the dynamical information contained in the collinearity-angle distribution.

(vii) The results at  $W=7$  GeV are shown in Fig. 8. Here we also show the distributions for the case  $M_L=2.8$  GeV and  $M_{\nu_L}=1.4$  GeV [see Eq. (2.19)]. We see that the effects of the second set of heavy leptons (2.19) on the  $e\mu$  cross section would be small even if they exist. At those energies, the analytical formula given in Ref. 14 can give a good qualitative description of the collinearity-angle distribution at small values of  $\theta$ , where the effects of the finite energy cutoff are small.

Finally, we would like to note that  $V-A$  and  $V+A$  couplings gave rise to the different energy spectra in (3.3) and the different collinearity-angle distributions in (3.8) just because we assumed a parity-violating current for the ordinary leptons  $e$  and  $\mu$ , namely, a  $V-A$  current in the Lagrangian (1.1). If one assumes a  $V+A$  current for the ordinary leptons, which appears rather unlikely but is not *a priori* excluded when the ordinary leptons couple to the heavy lepton, the role of  $V-A$  and  $V+A$  couplings for the heavy lepton in these distributions is interchanged. Namely, the parameter  $\alpha$  in Eqs. (3.3) and (3.8) is replaced by  $\frac{1}{2}\pi - \alpha$ , and a  $V-A$  current for the heavy lepton gives rise

to more  $e\mu$  events at smaller values of  $\theta$  than a  $V+A$  current. In this sense, one cannot determine the absolute structure of the heavy-lepton current on the basis of the energy spectrum and collinearity-angle distribution alone. These considerations also apply to the  $l\pi$  events to be discussed in Sec. IV.

#### IV. $l\pi$ EVENTS

From Table I, we observe that the simplest decay mode

$$L \rightarrow \nu_L + \pi \quad (4.1)$$

is relatively important for the heavy lepton with a mass of  $\sim 1.8$  GeV. The relative decay rate for (4.1) also rapidly increases when the mass of  $\nu_L$  becomes nonzero. These properties, which are characteristic of  $V$  and  $A$  couplings, can be utilized to check the dynamics. Moreover, the energy spectrum of the pion in (4.1) is uniformly distributed over the phase space

$$\frac{d\Gamma}{dx} = \frac{1}{\beta(1-\epsilon^2)} \text{ for } \frac{1-\epsilon^2}{2}(1-\beta) \leq x \leq \frac{1-\epsilon^2}{2}(1+\beta). \quad (4.2)$$

See Eqs. (3.1) and (3.2) for the definition of various parameters. This property of the pion spectrum may be conveniently used to fix the mass of  $\nu_L$ , which is needed to discriminate  $V-A$  and  $V+A$  couplings.

We are thus motivated to investigate the  $l\pi$  events<sup>15</sup>

$$e\bar{e} \rightarrow L\bar{L} \rightarrow (\nu_L + l + \bar{\nu}_l) + (\bar{\nu}_L + \pi) \\ \rightarrow (\nu_L + \pi) + (\bar{\nu}_L + \bar{l} + \nu_l), \quad (4.3)$$

with  $l=\mu$  or  $e$  (see Fig. 9). The lepton spectrum in (4.3) is the same as in  $e\mu$  events. The collinearity-angle distributions for  $l$  and  $\pi$  can be evaluated on the basis of a similar set of assumptions that we made in Sec. III. In particular, we neglect the pion mass.

The normalized distribution for  $l$  and  $\pi$  in Fig. 9 is given by

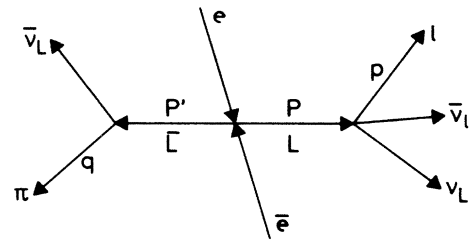


FIG. 9.  $l\pi$  production ( $l=\mu$  or  $e$ ) via a heavy-lepton pair in  $e\bar{e}$  annihilation. The collinearity angle  $\theta$  is defined by  $\cos\theta \equiv -(\vec{p} \cdot \vec{q})/|\vec{p}||\vec{q}|$ .



$$d\Gamma = \frac{1}{N} (T_1 + T_2) \left( \frac{s - m^2}{s} \right) \frac{d^3 p}{2p_0} \frac{d^3 q}{2q_0} \times \delta((P - p)^2 - s) \delta((P' - q)^2 - m^2) ds. \quad (4.4)$$

The matrix elements  $T_1$  and  $T_2$  corresponding to the Lagrangian (1.1) and Eq. (2.2) are given by

$$T_1 = \left( \frac{W^2 + 2M^2}{2M^2} \right) F(s), \quad (4.5)$$

$$T_2 = \frac{4 \cos 2\alpha}{1 - \epsilon^2} \frac{G(s)}{M^2} \times \left[ M^2(p \cdot q) - (P' \cdot p)(P' \cdot q) - (P \cdot p)(P \cdot q) + \left( \frac{W^2 - 2M^2}{2M^2} \right) (P \cdot p)(P' \cdot q) \right], \quad (4.6)$$

where  $F(s)$  and  $G(s)$  are defined in (3.11) and (3.12), respectively. The natural phase-space boundary in (4.4) is

$$m^2 \leq s \leq M^2. \quad (4.7)$$

The normalization factor  $N$  is given by

$$N = \left( \frac{W^2 + 2M^2}{2M^2} \right) \left( \frac{\pi M^6}{24} \right) \left[ \frac{1}{2} \pi (1 - \epsilon^2) \right] \times [f(\epsilon) + \sin 2\alpha g(\epsilon)], \quad (4.8)$$

with  $f(\epsilon)$  and  $g(\epsilon)$  in (3.5) and (3.6), respectively. In (4.4)  $T_2$  stands for spin-alignment term. Note that  $T_2$  vanishes for  $|\alpha| = \frac{1}{4}\pi$ , namely, for a pure  $V$  or  $A$  current for the heavy lepton. The collinearity-angle distributions obtained from (4.4) at  $W = 4.8$  GeV with suitable energy cutoffs,

$$p_0 \geq E_c \text{ and } q_0 \geq E'_c, \quad (4.9)$$

are shown in Figs. 10 and 11. Here we allow the different cutoff energies for  $l$  and  $\pi$ . See Appendix A for the phase-space constraints. The character-

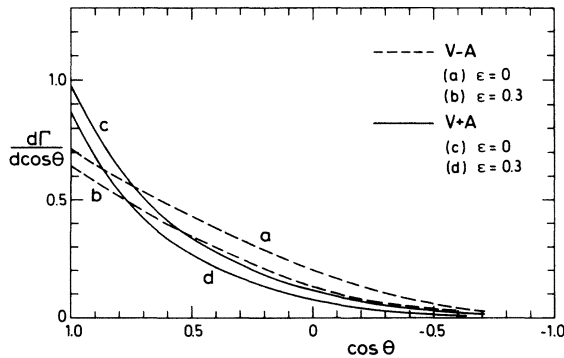


FIG. 10. Collinearity-angle distribution of  $l$  and  $\pi$  for  $M = 1.8$  GeV and  $W = 4.8$  GeV. The cutoff energy is taken at  $E_c = 0.65$  GeV both for  $l$  and  $\pi$ . Also  $\epsilon = m_{\nu_L}/M$ .

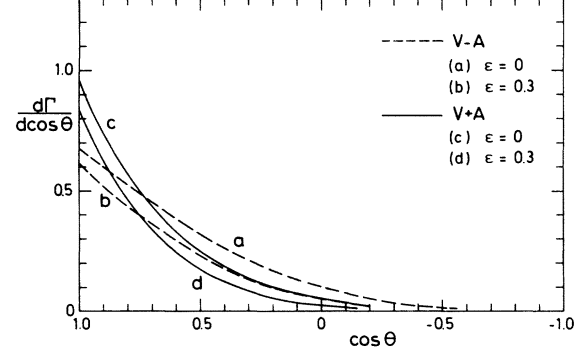


FIG. 11. Collinearity-angle distribution of  $l$  and  $\pi$  for  $M = 1.8$  GeV and  $W = 4.8$  GeV. The cutoff energy for  $l$  is taken at  $0.65$  GeV and that for  $\pi$  at  $1.0$  GeV. Also,  $\epsilon = m_{\nu_L}/M$ .

istic features of these distributions are as follows:

(i) A  $V+A$  current again tends to give rise to smaller values of the collinearity angle  $\theta$  compared with a  $V-A$  current. The difference between  $V-A$  and  $V+A$  currents is even more pronounced in the present case than in  $e\mu$  events. The effects of the nonvanishing neutrino mass are also similar to those in  $e\mu$  events.

(ii) The fraction  $f$  of the  $l\pi$  events defined in (3.16) is still substantial even with a cutoff energy for the pion at  $E'_c = 1$  GeV (see Fig. 11). Namely

$$2 \times f = 0.75 \text{ and } 0.69 \quad (4.10)$$

for  $V-A$  and  $V+A$  couplings with  $\epsilon = 0$ , respectively. The factor 2 in (4.10) arises from the two possibilities,  $l = \mu$  or  $e$ . Combined with the substantial branching ratio for (4.1), this property may make it easy to measure  $l\pi$  events, in particular, when the neutrino  $\nu_L$  is massive [cf. Eq. (3.17)].

An analytic formula for the  $l\pi$  events is discussed in Appendix B.

*Note added.* After completing the present work, a related work by S.-Y. Pi and A. I. Sanda [Phys. Rev. Lett. 36, 1 (1976); 36, 453 (1976) (E)] came to our attention. Their conclusion concerning the  $e\mu$  events is similar to ours.

#### ACKNOWLEDGMENTS

We thank our colleagues both at the Institute for Nuclear Study, University of Tokyo, and DESY, Hamburg, for stimulative discussions. We also thank Professor H. Joos and Dr. T. Walsh for reading the manuscript and for making very useful comments.

## APPENDIX A

Here we briefly summarize the phase-space constraints. The masses of the electron, muon, and pion are all neglected. We discuss only the case of Eq. (3.8), but essentially identical considerations apply to Eq. (4.4) as well. One can first integrate over the energy variables  $p_0$  and  $q_0$  by using the  $\delta$  functions in (3.8). The natural phase-space boundaries (3.14) are modified to

$$m^2 \leq s \leq M^2 - 2M\gamma E_c(1-\beta Z), \quad (\text{A1})$$

$$m^2 \leq s' \leq M^2 - 2M\gamma E'_c(1-\beta Z') \quad (\text{A2})$$

for fixed angular variables  $Z$  and  $Z'$  when one imposes the energy cutoffs

$$E_c \leq p_0 \text{ and } E'_c \leq q_0. \quad (\text{A3})$$

Here the variables  $Z$  and  $Z'$  are defined by (see also Fig. 2)

$$Z \equiv (\vec{p} \cdot \vec{P}) / |\vec{p}| |\vec{P}| \text{ and } Z' \equiv (\vec{q} \cdot \vec{P}') / |\vec{q}| |\vec{P}'|. \quad (\text{A4})$$

$M$ ,  $\beta$ , and  $\gamma$  are the mass and Lorentz factors of  $L$ , respectively, and  $m$  is the mass of  $\nu_L$ . In terms of the collinearity angle  $\theta$  in (3.15),  $Z'$  can be written as

$$Z' = Z \cos \theta + (1 - Z^2)^{1/2} \sin \theta \cos \phi. \quad (\text{A5})$$

when one integrates over  $s$  and  $s'$  within the boundaries (A1) and (A2), the remaining phase space is proportional to

$$dZ d\phi \cos \theta. \quad (\text{A6})$$

The collinearity angle  $\theta$  is limited by

$$0 \leq \theta \leq \min[\pi, \cos^{-1} Z_c + \cos^{-1} Z'_c], \quad (\text{A7})$$

where

$$Z_c \equiv \max \left\{ \frac{1}{\beta\gamma} \left[ \gamma - \frac{M}{2E_c} (1-\epsilon^2) \right], -1 \right\}, \quad (\text{A8})$$

$$Z'_c \equiv \max \left\{ \frac{1}{\beta\gamma} \left[ \gamma - \frac{M}{2E'_c} (1-\epsilon^2) \right], -1 \right\},$$

with  $\epsilon \equiv m/M$ . For fixed  $\theta$ , one can integrate over  $\phi$  and  $Z$  within the boundaries

$$|\phi| \leq \min \left[ \pi, \cos^{-1} \left( \frac{Z'_c - Z \cos \theta}{(1-Z)^{1/2} \sin \theta} \right) \right] \quad (\text{A9})$$

and

$$Z_c \leq Z \leq 1.$$

In Eqs. (A7)–(A9), min and max stand for the minimum and maximum, respectively. The last two integrations have been performed numerically in our study.

## APPENDIX B

The collinearity-angle distribution for the  $l\pi$  events without any energy and angular cutoffs can be written at threshold  $W=2M$  as

$$\frac{d\Gamma}{d\cos\theta} = \frac{1}{2} \left[ 1 + \frac{1}{3} \eta(\epsilon, \alpha) \cos \theta \right], \quad (\text{B1})$$

where the parameter  $\eta(\epsilon, \alpha)$  on the basis of the Lagrangian (1.1) is given by

$$\eta(\epsilon, \alpha) = \cos 2\alpha \left[ \frac{\cos^2 \alpha f(\epsilon) + \sin^2 \alpha h(\epsilon) + \sin 2\alpha g(\epsilon)}{f(\epsilon) + \sin 2\alpha g(\epsilon)} \right], \quad (\text{B2})$$

with

$$h(\epsilon) = \frac{1}{3} \left[ (1-\epsilon^2)(1-11\epsilon^2-47\epsilon^4-3\epsilon^6) - 12\epsilon^4(3+2\epsilon^2)\ln\epsilon \right], \quad (\text{B3})$$

and  $f(\epsilon)$  and  $g(\epsilon)$  defined in (3.5) and (3.6), respectively. For  $\epsilon = m/M = 0$ , we have

$$\eta(0, 0) = 1 \text{ for } V+A, \quad (\text{B4})$$

$$\eta(0, \frac{1}{2}\pi) = -\frac{1}{3} \text{ for } V-A. \quad (\text{B5})$$

The corresponding parameters for the  $e\mu$  events discussed in Ref. 14 are  $\eta(0, 0) = 1$  and  $\eta(0, \frac{1}{2}\pi) = \frac{1}{3}$ , respectively. The asymmetry between  $V+A$  and  $V-A$  is larger in the  $l\pi$  events than in the  $e\mu$  events. The analytic formula for the  $e\mu$  events given in Ref. 14 is also applicable to the  $l\pi$  events if one replaces  $\eta(\epsilon)$  in Ref. 14 by  $\eta(\epsilon, \alpha)$  in (B2). The scaling property discussed there also holds for the  $l\pi$  events at high energies, and asymmetry between  $V+A$  and  $V-A$  will be relatively large at PEP and PETRA energies, e.g.,  $W = 20\text{--}30$  GeV.

\*Permanent address: Institute for Nuclear Study, University of Tokyo, Tanashi, Tokyo 188, Japan.

<sup>1</sup>M. L. Perl *et al.*, Phys. Rev. Lett. 35, 1489 (1975); M. L. Perl, Lectures on Electron-Positron Annihilation, part II, SLAC Report No. SLAC-PUB-1592, 1975 (unpublished).

<sup>2</sup>A good review of earlier works on heavy leptons is found in M. L. Perl and P. Rapisarda, SLAC Report No. SLAC-PUB-1496, 1974 (unpublished). For earlier

experimental searches for  $e\mu$  events, see S. Orito *et al.*, Phys. Lett. 48B, 165 (1974) and references therein. The importance of heavy leptons in understanding the increasing ratio  $R$  in  $e\bar{e}$  annihilation was emphasized by a number of people, two of whom were J. J. Sakurai, in *Proceedings of the 1971 International Symposium on Electron and Photon Interactions at High Energies*, edited by N. B. Mistry (Laboratory of Nuclear Studies, Cornell University, Ithaca, New York,

- 1972), p. 49, and J. D. Bjorken, in *Proceedings of the Sixth International Symposium on Electron and Photon Interactions at High Energies, Bonn, Germany, 1973*, edited by H. Rollnik and W. Pfeil (North-Holland, Amsterdam, 1974), p. 25.
- <sup>3</sup>K. Fujikawa and N. Kawamoto, *Phys. Rev. Lett.* **35**, 1560 (1975).
- <sup>4</sup>Gauge models of a simple group structure are summarized in J. D. Bjorken and C. H. Llewellyn Smith, *Phys. Rev. D* **7**, 887 (1973). See also B. C. Barish *et al.*, *Phys. Rev. Lett.* **32**, 1387 (1974).
- <sup>5</sup>A. K. Mann, *Lett. Nuovo Cimento* **1**, 486 (1971); J. J. Sakurai, *ibid.* **1**, 624 (1971); E. W. Beier, *ibid.* **1**, 1118 (1971); H. B. Thacker and J. J. Sakurai, *Phys. Lett.* **36B**, 103 (1971); Y. S. Tsai, *Phys. Rev. D* **4**, 2821 (1971) and references quoted therein. See also Ref. 4 above.
- <sup>6</sup>S. Weinberg, *Phys. Rev. Lett.* **18**, 507 (1967).
- <sup>7</sup>T. Das, V. S. Mathur, and S. Okubo, *Phys. Rev. Lett.* **18**, 76 (1967).
- <sup>8</sup>See, e.g., R. E. Marshak *et al.*, *Theory of Weak Interactions in Particle Physics* (Wiley, New York, 1969).
- <sup>9</sup>B. Richter, in *Proceedings of the XVII International Conference on High Energy Physics, London, 1974*, edited by J. R. Smith (Rutherford Laboratory, Chilton, Didcot, Berkshire, England, 1974), p. IV-37. See also F. J. Gilman, SLAC Report No. SLAC-PUB-1537, 1975 (unpublished).
- <sup>10</sup>R. Schwitters, in *Proceedings of the 1975 International Symposium on Lepton and Photon Interactions at High Energies, Stanford, California, 1975*, edited by W. T. Kirk (SLAC, Stanford, 1976), p. 5. See also F. Gilman, p. 131 in the same proceedings.
- <sup>11</sup>J.-E. Augustin *et al.*, *Phys. Rev. Lett.* **34**, 764 (1975).
- <sup>12</sup>G. Feldman, in *Proceedings of the 1975 International Symposium on Lepton and Photon Interactions at High Energies, Stanford, California, 1975*, edited by W. T. Kirk (SLAC, Stanford, 1975), p. 39.
- <sup>13</sup>Y. S. Tsai, *Phys. Rev. D* **4**, 2821 (1971); S. Kawasaki, T. Shirafuji, and S. Y. Tsai, *Prog. Theor. Phys.* **49**, 1656 (1973).
- <sup>14</sup>K. Fujikawa and N. Kawamoto, *Phys. Rev. D* **13**, 2534 (1976).
- <sup>15</sup>The importance of this process was also commented on by T. C. Yang [*Lett. Nuovo Cimento* (to be published)]. As for the collinearity-angle distribution, see the second paper in Ref. 13.